Synthesis of a Highly Reactive Form of WO_2Cl_2, its Conversion into Nanocrystalline Mono-Hydrated WO_3 and Coordination Compounds with Tetramethylurea

Marco Bortoluzzi,[a] **Claudio Evangelisti,**[b] **Fabio Marchetti,***[c] **Guido Pampaloni,**[c] **Fabio Piccinelli,**[d] **Stefano Zacchini** [e]

[a] *Università di Venezia Ca' Foscari, Dipartimento di Scienze Molecolari e Nanosistemi, Via Torino 155, I-30170 Mestre (VE), Italy.*
[b] *Istituto di Scienze e Tecnologie Molecolari (ISTM-CNR), Via G. Fantoli 16/15, I-20138 Milano, Italy.*
[c] *Università di Pisa, Dipartimento di Chimica e Chimica Industriale, Via Moruzzi 13, I-56124 Pisa, Italy. Tel: +39 050 2219245. E-mail: fabio.marchetti1974@unipi.it. Webpage: http://www.dcci.unipi.it/fabio-marchetti.html.*
[d] *Università di Verona, Dipartimento di Biotecnologie, Laboratorio di Chimica dello Stato Solido, Strada Le Grazie 15, I-37134 Verona, Italy.*
[e] *Università di Bologna, Dipartimento di Chimica Industriale "Toso Montanari", Viale Risorgimento 4, I-40136 Bologna, Italy.*

This submission was created using the RSC Article Template (DO NOT DELETE THIS TEXT)
(LINE INCLUDED FOR SPACING ONLY - DO NOT DELETE THIS TEXT)

A new form of WO_2Cl_2 was obtained by a modification of a literature procedure. Both the newly prepared WO_2Cl_2 and the commercial yellow WO_2Cl_2 exhibited orthorhombic structure (powder X-ray diffraction, P-XRD), and their air exposure at room temperature afforded light green and lemon yellow $WO_3 \cdot H_2O$ (orthorhombic phase), respectively. These materials were characterized by P-XRD, high-resolution transmission electron microscopy (HR-TEM) and scanning transmission electron microscopy (S-TEM). The analyses revealed the nanocrystalline nature of light green $WO_3 \cdot H_2O$, and the prevalent amorphism of lemon yellow $WO_3 \cdot H_2O$. The reactions of grey WO_2Cl_2 with one and two equivalents of tetramethylurea (tmu), in CH_2Cl_2 at room temperature, led to the isolation of the trinuclear complex $[WO_2Cl_2(tmu)]_3$, **1** (45% yield), and the mononuclear one $WO_2Cl_2(tmu)_2$, **2** (64%), respectively. Compounds **1** and **2** were fully characterized by analytical and spectroscopic methods, single crystal X-ray diffraction (SC-XRD) and DFT calculations.

Introduction

Tungsten(VI) dioxide dichloride, WO_2Cl_2, has aroused a considerable interest due to the possible applications in solid state chemistry [1] and as a catalytic precursor for a variety of organic transformations.[2] On the other hand, as an air sensitive, oxophilic metal chloride, WO_2Cl_2 is a potential precursor for the deposition of films of the corresponding metal oxide, WO_3.[3] The latter is hugely investigated in view of technological applications, and indeed there is currently high interest in developing suitable methods for the production of WO_3-based thin films.[4]
WO_2Cl_2 can be efficiently obtained as yellow flakes by WO_3/WCl_6 metathesis, performed in a sealed tube at high temperature.[5] A more convenient laboratory method, affording a yellow solid, was published in 1990, and consisted in the reaction of $WOCl_4$ with hexamethyldisiloxane in octane at 80 °C (Eqn. 1).[6] It should be remarked also that several chemical suppliers have yellow-WO_2Cl_2 in their product catalogues.

$$WOCl_4 + O(SiMe_3)_2 \rightarrow WO_2Cl_2 + 2ClSiMe_3 \qquad (1)$$
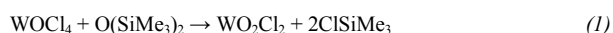
The structure of WO_2Cl_2 was previously investigated by single crystal X-ray diffraction and powder neutron diffraction experiments.[7] The structure revealed to be orthorhombic (space group *Immm*), showing sheets of rectangular WO_4 units spaced by layers of chloride anions.[7a]
The polymeric network of WO_2Cl_2 may be cleaved by the addition of group 15 and group 16 donor ligands, leading to the formation of mononuclear metal compounds.[8]
In the framework of our interest in the chemistry of high valent transition metal halides,[9] herein we report the straightforward synthesis of a new form of WO_2Cl_2, obtained by a modification of the literature procedure (Eqn. 1).[6] A comparative description will

be provided of the hydrolytic conversion into WO_3 of novel and commercially available WO_2Cl_2, respectively.
Furthermore, we were interested to check whether the oxidative chemistry of WCl_6 towards some classes of organic compounds could be extended to WO_2Cl_2. In particular, WCl_6 may act as a monoelectron abstractor from tetraalkylureas [10] and amines,[11] thus promoting unusual activation pathways through the intermediate formation of radical cation species. On considering that the reactivity of tungsten(VI) dioxide dichloride with alkylureas has never been described heretofore, the reactions of WO_2Cl_2 with limited amounts of tetramethylurea (tmu) were studied in a weakly coordinating medium (dichloromethane).

Results and Discussion

WO_2Cl_2 was obtained as a light grey solid in 75% yield, by the direct reaction of WCl_6 with two equivalents of hexamethyldisiloxane in heptane at 80 °C (Eqn. 2).

$$WCl_6 + 2O(SiMe_3)_2 \rightarrow WO_2Cl_2 + 4Me_3SiCl \qquad (2)$$
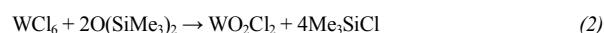
A tentative explanation of the different outcomes of the reactions reported in Equations 1) and 2), respectively, is that the direct synthesis of WO_2Cl_2 from WCl_6 (Eqn. 2) might not proceed via the intermediacy of $WOCl_4$ (Eqn. 1).
The isolated material (Eqn. 1) was characterized by Cl elemental analysis, IR spectroscopy and P-XRD diffraction. The IR spectrum (solid state) displays strong bands centred at 846, 800 and 760 cm^{-1}, ascribable to the [W=O] moieties within the polynuclear structure.[6]
The P-XRD pattern was recorded by protecting the sample from the air with a thin layer of inert paraffin oil, and resulted consistent with the presence of orthorhombic WO_2Cl_2 (*Immm* space group), see Figure S1 within the Supporting Information. The presence of traces

of impurities, possibly contributing to the grey colour, could not be definitely ruled out. The orthorhombic structure was detected also for the commercial (Sigma Aldrich), yellow WO_2Cl_2, in agreement with previous findings (see Introduction).[7] The P-XRD pattern of yellow WO_2Cl_2 is shown in Figure S1; the related transmission electron micrographs revealed the presence of large WO_2Cl_2 crystals (Figure S2). Figure 1 compares a commercial sample of WO_2Cl_2 (Sigma Aldrich, 99%) with a sample obtained according to Eqn. 2.
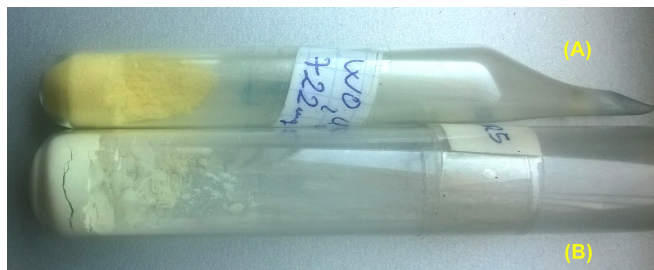

Figure 1. Samples of WO_2Cl_2: (A) commercial; (B) prepared according to Eqn. 2.

Although the two forms of WO_2Cl_2, i.e. grey and yellow, display orthorhombic structure, they exhibit considerably different behaviours when allowed to contact with air.[12] This feature might be ascribable to a difference in the average size of the respective crystalline domains in the two solid materials.[13] Thus, grey WO_2Cl_2 was found to be much more sensitive than the homologous yellow material. Indeed, in the absence of oil protection, rapid degradation of the sample of grey WO_2Cl_2 could be monitored by P-XRD (Figure S3). The degradation was fast and complete in less than one hour from air exposure, resulting in the formation of a light-green solid.[14] Otherwise, the P-XRD peaks related to the orthorhombic phase (*Immm*) were the only ones detected after two hours from air exposure of the yellow WO_2Cl_2 sample; complete degradation of this compound required 72 h, affording a lemon yellow solid (Figure S3). We obtained analogous solid compounds in the laboratory, by allowing the two forms of WO_2Cl_2, respectively, to keep in contact with moist air for 3 days. The resulting products contained only traces of chlorine, thus indicating the occurrence of prevalent hydrolysis (Eqn. 3). They were both identified as $WO_3 \cdot H_2O$ by means of P-XRD and electron microscopy analyses.

$$WO_2Cl_2 + 2H_2O \rightarrow WO_3 \cdot H_2O + 2HCl \qquad (3)$$
grey   *light-green*
yellow   *lemon yellow*
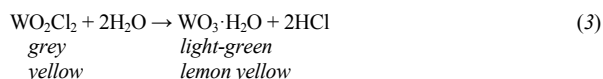
The P-XRD pattern related to light-green $WO_3 \cdot H_2O$ (from grey WO_2Cl_2, see Eqn. 3) indicated the presence of nanocrystalline $WO_3 \cdot H_2O$ (orthorhombic *Pmnb* space group, Figure 2), the estimated average crystal size being 9(1) nm. High-resolution transmission electron microscopy (HR-TEM) and scanning transmission electron microscopy (S-TEM) analyses were in agreement with the P-XRD data. They showed partially rolled nanosheets containing small nanocrystalline domains ranging in size between 3 and 10 nm (Figures 3 and S4); the electron-diffraction patterns were successfully indexed on the basis of $WO_3 \cdot H_2O$ structure (orthorhombic unit cell, $a = 0.5235$ nm, $b = 1.0688$ nm and $c = 0.5123$ nm).[15]

The P-XRD pattern collected for lemon yellow $WO_3 \cdot H_2O$ (from yellow WO_2Cl_2, see Eqn. 3) showed a lower degree of crystallinity compared to light-green $WO_3 \cdot H_2O$ (from grey WO_2Cl_2, Figure S3). The presence of large amount of an amorphous phase was confirmed by HR-TEM analysis (Figure S5).
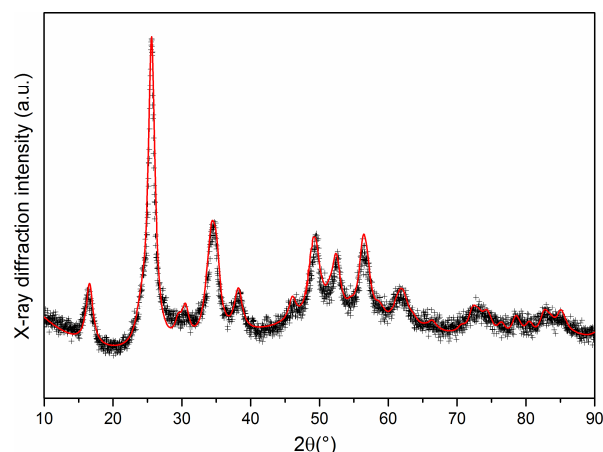

Figure 2. Observed X-ray pattern (black crosses) and Rietveld refinement (red solid line) of the solid obtained from grey WO_2Cl_2 upon air exposure for 3 days. The structural model used for the refinement was the orthorhombic phase of $WO_3 \cdot H_2O$ (space group *Pmnb*, PDF card 04-011-6930). Final $R_w = 8.02\%$.

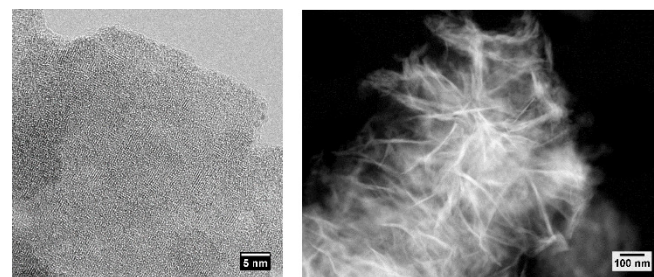**Figure 3**. Representative HRTEM (*left side*) and STEM (*right side*) micrographs of light-green $WO_3 \cdot H_2O$ derived from grey WO_2Cl_2.

To the best of our knowledge, the non incidental formation of tungsten oxide from WO_2Cl_2 is reported here for the first time.[16] It has to be noted that the hydrolytic conversion of high valent metal oxide halides to metal oxides might be a complicated issue.[17]

The faster hydrolytic degradation of grey WO_2Cl_2, compared to that of the traditional, yellow WO_2Cl_2, suggested us that the former may be a preferential starting material for studying the reactivity with organic species. As a matter of fact, WO_2Cl_2 is known to be a quite inert polymeric substance,[8a,18] thus its coordination compounds have been more often prepared from molecular precursors, such as WCl_6 and $WO_2Cl_2(1,2$-dimethoxyethane),[19] rather than by direct addition of the ligands to WO_2Cl_2.[8,20]

We moved to study the reactivity of grey WO_2Cl_2 with stoichiometric amounts of tetramethylurea. The 1:1 molar reaction afforded a mixture of compounds, and a complex of formula $WO_2Cl_2(tmu)$ could be isolated in 45% yield by fractional crystallization (Scheme 1). SC-XRD analysis allowed us to identify this product as the trimer $[WO_2Cl_2(tmu)]_3$, **1** (Figure 4 and Table 1). The three W(VI) centres exhibit a distorted octahedral geometry, and are linked by three asymmetric μ-O ligands. These latter display a short π-bond to one W [1.753(6)-1.763(6) Å] and a longer bridging bond to the adjacent tungsten [2.211(6)-2.226(6) Å]. Complex **1** is a very rare polynuclear WO_2Cl_2 coordination complex, the only other example being the tetramer $[WO_2Cl_2(thf)]_4$.[21]
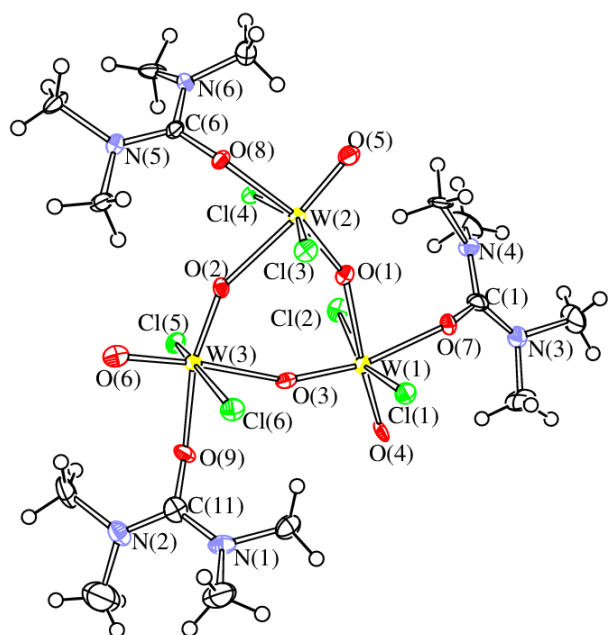
Figure 4. Molecular structure of **1**, with key atoms labelled. Thermal ellipsoids are at the 50% probability level. H-bonds are drawn with dashed lines.

Table 1. Selected bond distances (Å) and angles (°) for **1**.

W(1)–O(1)	2.220(6)	W(2)–O(1)	1.763(6)
W(2)–O(2)	2.226(6)	W(3)–O(2)	1.753(6)
W(3)–O(3)	2.211(6)	W(1)–O(3)	1.758(6)
W(1)–O(4)	1.774(7)	W(1)–O(7)	2.096(6)
W(2)–O(5)	1.701(7)	W(2)–O(8)	2.136(6)
W(3)–O(6)	1.725(7)	W(3)–O(9)	2.088(7)
W(1)–Cl(1)	2.321(3)	W(1)–Cl(2)	2.338(3)
W(2)–Cl(3)	2.324(2)	W(2)–Cl(4)	2.354(2)
W(3)–Cl(5)	2.347(2)	W(3)–Cl(6)	2.333(2)
C(1)–O(7)	1.297(11)	C(6)–O(8)	1.276(11)
C(11)–O(9)	1.287(12)	C(1)–N(3)	1.336(12))
C(1)–N(4)	1.317(12)	C(6)–N(5)	1.331(12)
C(6)–N(6)	1.347(12)	C(11)–N(1)	1.329(13)
C(11)–N(2)	1.315(14)		
O(1)–W(1)–O(4)	175.3(3)	O(3)–W(1)–O(7)	164.1(3)
O(1)–W(2)–O(8)	166.6(3)	O(5)–W(2)–O(2)	173.1(3)
O(2)–W(3)–O(9)	164.5(3)	O(3)–W(3)–O(6)	173.1(3)
Cl(1)–W(1)–Cl(2)	161.79(9)	Cl(3)–W(2)–Cl(4)	158.79(9)
Cl(5)–W(3)–Cl(6)	162.02(9)	W(1)–O(1)–W(2)	154.8(4)
W(2)–O(2)–W(3)	152.3(3)	W(3)–O(3)–W(1)	156.5(3)
W(1)–O(7)–C(1)	136.9(7)	W(2)–O(8)–C(6)	137.0(6)
W(3)–O(9)–C(11)	141.6(7)	Sum at C(1)	360.0(16)
Sum at C(6)	359.9(16)	Sum at C(11)	360.0(11)

The DFT calculated structure of **1** is depicted in Figure 5, together with the corresponding electron density surface (selected bonding parameters are given in the caption). Also the geometry of the hypothetical WO$_2$Cl$_2$(tmu) monomer (**1-mono**) was optimized at DFT level, and this is shown in the inset of Figure 5; **1-mono** possesses distorted square pyramidal geometry. From a thermodynamic point of view, the hypothetical oligomerization of **1-mono** to give **1** is a strongly exergonic process (Eqn. 4).
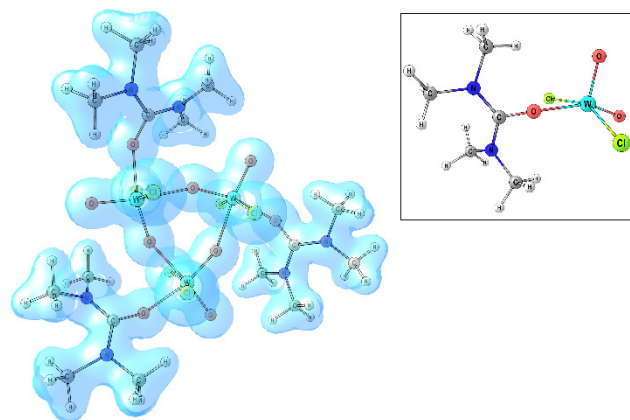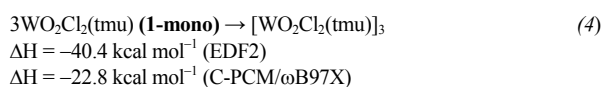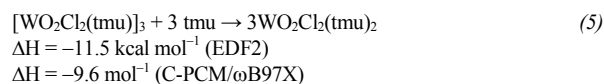
3WO$_2$Cl$_2$(tmu) (**1-mono**) → [WO$_2$Cl$_2$(tmu)]$_3$ *(4)*
ΔH = −40.4 kcal mol^{-1} (EDF2)
ΔH = −22.8 kcal mol^{-1} (C-PCM/ωB97X)

Figure 5. DFT calculated structure of **1** with electron density surface (isovalue = 0.05 a.u.). Inset: structure of **1-mono**. Selected computed average bond lengths for **1** (Å, C-PCM/ωB97X, corresponding EDF2 data in parenthesis): W=O(terminal) 1.677 (1.710); W=O(bridging) 1.731 (1.762); W–O(bridging) 2.263 (2.229); W–O(tmu) 2.093 (2.138); W–Cl 2.360 (2.368). Selected computed average bond lengths for **1-mono** (Å, C-PCM/ωB97X, corresponding EDF2 data in parenthesis): W=O(axial) 1.674 (1.705); W=O(equatorial) 1.689 (1.707); W–O(tmu) 2.096 (2.172); W–Cl 2.370 (2.355).

The quite different electron densities exhibited by **1** along the different W–O bonds prompted us to study these bonds by means of Mayer bond order analysis (Table S1). As expected, the highest orders refer to the terminal W=O bonds, while the bond order calculated for the bridged W=O units is about 25% lower. The partial loss of multiple bond character is accompanied by an increase of the negative partial charge on the oxygen atoms. Thus, the average Mulliken charge is −0.515 a.u. on the terminal oxide ligands (C-PCM/ωB97X; −0.541 a.u. at EDF2 level), and −0.688 a.u. on the μ-O atoms (−0.690 a.u. at EDF2 level).

Salient IR data of **1** (solid state) are represented by two absorptions at 1575 and 1531 cm^{-1}, that have been attributed to mixed C=O and C–N stretching vibrations, with the assistance of DFT simulations.

The 1:2 molar reaction of WO$_2$Cl$_2$ with tmu afforded the monomeric complex WO$_2$Cl$_2$(tmu)$_2$, **2**, in 64% yield. Computed thermodynamic data indicate that the conversion of **1** to **2** upon tmu addition should be a highly favourable process (Eqn. 5).

[WO$_2$Cl$_2$(tmu)]$_3$ + 3 tmu → 3WO$_2$Cl$_2$(tmu)$_2$ *(5)*
ΔH = −11.5 kcal mol^{-1} (EDF2)
ΔH = −9.6 mol^{-1} (C-PCM/ωB97X)

Compound **2** represents a non common case of a crystallographically characterized WO$_2$Cl$_2$L$_2$ complex, where L is a monodentate ligand (Figure 6, Table 2).[20b,22] Coherently with the π-character, the W(1)–O(1) [1.684(10) Å] and W(1)–O(2) [1.718(9) Å] bonds are considerably shorter than W(1)–O(3) [2.194(8) Å] and W(1)–O(4) [2.172(8) Å], the latter showing a pure coordinative nature. The computed Mayer bond orders for the W=O interactions are 1.909 and 1.936, *i.e.* comparable to the average value found for the terminal W=O bonds in **1** (1.933, see Table S1). On the other hand, the W–tmu Mayer bond orders in **2** are 0.369 and 0.397, meaningfully lower than the average value obtained for **1**, 0.507. The weaker coordination of tmu in **2** with respect to **1** can be explained on the basis of a reduced *trans*-influence of the bridging oxide ligands. The DFT-optimized geometry of **2** is supplied as Figure S6. The IR spectrum of **2** (solid state) displays a diagnostic absorption at 1540 cm^{-1}, due to mixed C=O and C–N stretching vibrations.
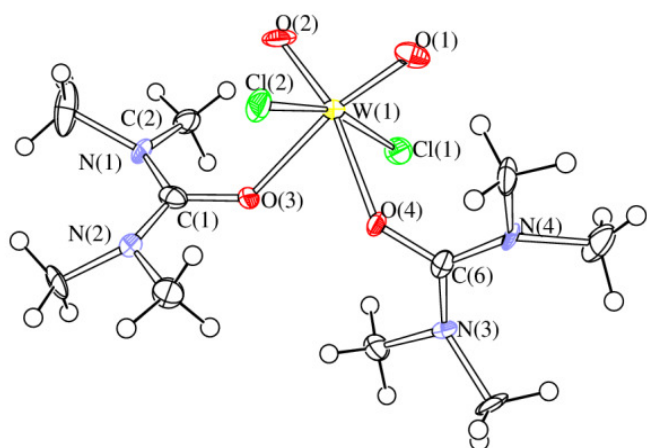
3

Figure 6. Molecular structure of **2**, with key atoms labelled. Thermal ellipsoids are at the 50% probability level.

Table 2. Selected bond distances (Å) and angles (°) for **2**.

W(1)–O(1)	1.684(10)	W(1)–O(2)	1.718(9)
W(1)–O(3)	2.194(8)	W(1)–O(4)	2.172(8)
W(1)–Cl(1)	2.385(3)	W(1)–Cl(2)	2.357(4)
C(1)–O(3)	1.311(15)	C(6)–O(4)	1.281(14)
C(1)–N(1)	1.334(17)	C(1)–N(2)	1.323(17)
C(6)–N(3)	1.313(17)	C(6)–N(4)	1.358(17)
O(1)–W(1)–O(3)	168.7(4)	O(2)–W(1)–O(4)	164.2(4)
Cl(1)–W(1)–Cl(2)	163.83(12)	O(1)–W(1)–O(2)	101.2(4))
O(3)–W(1)–O(4)	74.6(3)	W(1)–O(3)–C(1)	132.6(8)
W(1)–O(4)–C(6)	136.2(8)	Sum at C(1)	360(2)
Sum at C(6)	360(2)		

The synthesis of W(VI) coordination complexes from the reactions of WO$_2$Cl$_2$ with different ratios of tetramethylurea contrasts with what observed for the WCl$_6$/tmu reaction system. In the latter case, the presumable, initial formation of the tmu radical cation besides [WCl$_6$]$^-$ is followed by C–H activation and intermolecular H-migration, leading to the isolation of a protonated urea salt in moderate yield (Scheme 1).[10]
The absence of electron interchange between WO$_2$Cl$_2$ and tmu indicates that the presence of two oxide ligands significantly weakens the oxidative power of the W(VI) metal centre.[11,23]
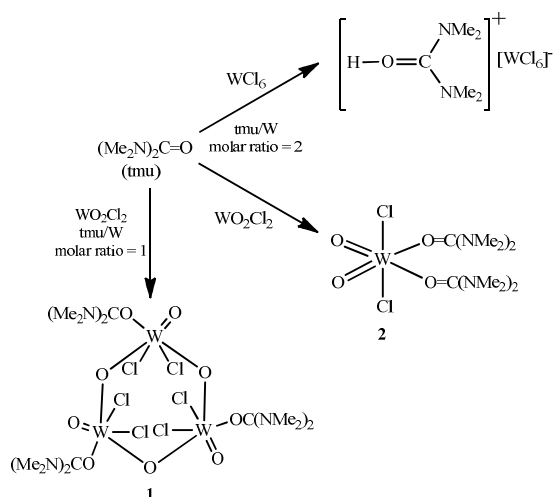
Scheme 1. Formation of coordination complexes from the reactions of WO$_2$Cl$_2$ with tmu, and a comparison with the parallel chemistry of WCl$_6$.[10]

Interestingly, the 1:1 molar reaction of yellow WO$_2$Cl$_2$ with tmu was slightly less selective respect to the analogous reaction performed using the homologous grey material (Scheme 1). A light green precipitate was recovered from the dichloromethane reaction

mixture. IR analysis of this solid evidenced the presence of three bands in the carbonyl region (1762, 1649, 1609 cm^{-1}), other than the absorptions due to **1**.

Conclusions

A modification of the known laboratory procedure allowed us to obtain a new form of WO$_2$Cl$_2$ as a light grey solid. Instead, the yellow colour is that typical of commercial WO$_2$Cl$_2$. The hydrolytic degradation of "grey" WO$_2$Cl$_2$ upon air exposure proceeds fast at room temperature, affording nanocrystalline WO$_3$·H$_2$O (light green). Conversely, the yellow WO$_2$Cl$_2$ to WO$_3$·H$_2$O conversion is a slower process resulting in the formation of a partially amorphous material. The synthesis of tungsten oxide from WO$_2$Cl$_2$ was not reported previously. Grey and yellow WO$_2$Cl$_2$, respectively, show some difference even when allowed to interact with tetramethylurea (tmu), the reaction with grey WO$_2$Cl$_2$ appearing slightly more selective. Two coordination complexes were obtained by the reactions of grey WO$_2$Cl$_2$ with limited amounts of tmu, and crystallographically characterized, thus providing the first information available on the reactivity of WO$_2$Cl$_2$ with alkylureas.

Experimental

General. *Warning*: the metal products reported in this paper are highly moisture-sensitive, thus rigorously anhydrous conditions were required for the reaction and crystallization procedures. The reaction vessels were oven dried at 140°C prior to use, evacuated (10^{-2} mmHg) and then filled with argon. WCl$_6$ (Strem, 99.9%) and WO$_2$Cl$_2$ (Sigma Aldrich, 99%) were purchased and stored in sealed glass tubes under argon atmosphere. Once isolated, the metal products were conserved in sealed glass tubes under argon. The organic reactants were commercial products (Alfa Aesar) stored under argon atmosphere as received. Solvents (Sigma Aldrich) were distilled from appropriate drying agents before use. Infrared spectra were recorded in the 4000-650 cm^{-1} range at 298 K with a FT IR-Perkin Elmer Spectrometer, equipped with a UATR sampling accessory. NMR spectra were recorded at 298 K on a Bruker Avance II DRX400 instrument equipped with BBFO broadband probe. The chemical shifts for ^{1}H and ^{13}C were referenced to the non-deuterated aliquot of the solvent. The spectra were fully assigned *via* ^{1}H,^{13}C correlation measured through *gs*-HSQC and *gs*-HMBC experiments.[24] Carbon, hydrogen and nitrogen analyses were performed on Carlo Erba mod. 1106 instrument. The chloride content was determined by the Mohr method [25] on solutions prepared by dissolution of the solid in aqueous KOH at boiling temperature, followed by cooling to room temperature and addition of H$_2$SO$_4$ up to neutralization.

Synthesis of WO$_2$Cl$_2$. A suspension of WCl$_6$ (5.198 g, 13.11 mmol) in heptane (60 mL) was treated with O(SiMe$_3$)$_2$ (5.85 mL, 27.52 mmol). The mixture was stirred at 80 °C for 16 h. The resulting greenish grey precipitate was isolated, washed with hexane (2 x 30 mL) and dried in vacuo. Yield 2.82 g, 75%. Anal. Calcd for Cl$_2$O$_2$W: Cl, 24.73. Found: Cl, 24.61. IR (solid state): ν = 846s-sh, 800vs, 760s-sh (ν$_{W=O}$) cm^{-1}.

Synthesis of WO$_3$·H$_2$O. *General procedure*: WO$_2$Cl$_2$ (0.60 mmol) was layered over a watchglass and left in contact with air. A progressive colour change was observed. After 72 h, the resulting solid material was collected and then characterized by elemental analysis, TEM and P-XRD.
A) From grey WO$_2$Cl$_2$: light green solid, yield 94%. Anal. Calcd for H$_2$O$_4$W: H, 0.81; Cl, 0.00. Found: H, 1.08; Cl, 0.28.
B) From yellow WO$_2$Cl$_2$ (commercial): lemon yellow solid, yield 95%. Anal. Calcd for H$_2$O$_4$W: H, 0.81; Cl, 0.00. Found: H, 1.20; Cl, 0.36.

Reactions of WO₂Cl₂ with tetramethylurea (tmu): synthesis of [WO₂Cl₂(tmu)]₃, 1, and WO₂Cl₂(tmu)₂, 2. *General procedure*: Tetramethylurea (tmu) was added to grey WO_2Cl_2 suspended in CH_2Cl_2 (ca. 15 mL), and the resulting mixture was left stirring at room temperature for 5 d. Then the reaction solution was concentrated up to ca. 5 mL, layered with hexane and settled aside at −30 °C. The product was collected as a crystalline material after ca. 1 week.

[WO₂Cl₂(tmu)]₃, 1. Green solid, from WO_2Cl_2 (0.250 g, 0.872 mmol) and tmu (0.105 mL, 0.872 mmol). Yield 0.158 g, 45%. Anal. Calcd for $C_5H_{12}Cl_2N_2O_3W$: C, 14.91; H, 3.00; N, 6.95; Cl, 17.60. Found: C, 14.84; H, 3.05; N, 6.90; Cl, 17.45. IR (solid state): ν = 2962w, 2862w, 1575m and 1531s ($ν_{C=O} + ν_{CN}$), 1471m, 1425m, 1409m-s, 1399s, 1322m, 1267w, 1234m, 1165m, 1068w, 975w-m ($ν_{WO,terminal+bridging}$), 903w, 866vs ($ν_{WO,terminal+bridging}$), 762s, 747m-s, 730m, 700w-m cm⁻¹. ¹H NMR (CD₃CN): δ = 3.06 (s, CH₃) ppm. ¹³C NMR (CD₃CN): δ = 163.0 (C=O), 39.4 (CH₃) ppm.

WO₂Cl₂(tmu)₂, 2. Colourless solid, from WO_2Cl_2 (0.240 g, 0.837 mmol) and tmu (0.21 mL, 1.8 mmol). Yield 0.278 g, 64%. Anal. Calcd for $C_{10}H_{24}Cl_2N_4O_4W$: C, 23.14; H, 4.66; N, 10.79; Cl, 13.66. Found: C, 23.07; H, 4.74; N, 10.84; Cl, 13.50. IR (solid state): ν = 2960w, 2886w, 1540s-br ($ν_{C=O} + ν_{NCN}$), 1470w-m, 1420m, 1397s, 1325w-m, 1260w, 1235w, 1163m, 1067s, 1018s, 960vs ($ν_{O=W=O, symm}$), 915vs ($ν_{O=W=O, asymm}$), 873s, 798s, 765s, 746s cm⁻¹. ¹H NMR (CD₂Cl₂): δ = 2.99 (s, CH₃) ppm. ¹³C NMR (CD₂Cl₂): δ = 165.9 (C=O), 39.2 (CH₃) ppm.

TEM studies. Transmission electron microscopy (TEM) analyses were carried out with a ZEISS LIBRA 200FE HRTEM instrument, equipped with a FEG source operating at 200 kV and EDS probe for chemical analysis. The samples were prepared by vigorously rubbing the solid between two clean glass slides, then they were dispersed onto holey-carbon films supported on a copper grid (300 mesh) by adherence.[26]

P-XRD studies. Powder X-ray-diffraction patterns were measured with a Thermo ARL X´TRA powder diffractometer, operating in the Bragg-Brentano geometry and equipped with a Cu-anode X-ray source (K$_α$, λ =1.5418 Å), using a Peltier Si(Li) cooled solid state detector. The patterns were collected with a scan step of 0.03 ° and an exposure time of 15 s in the 20°-90° 2θ range. The phase identifications were performed with the PDF-4+ 2013 database provided by the International Centre for Diffraction Data (ICDD). The air-sensitive polycrystalline samples of WO_2Cl_2 were grounded in a mortar, transferred to a low-background sample holder for the data collection and then protected by a film of inert paraffin oil. Rietveld refinement calculations were performed on $WO_3·H_2O$ samples, in order to calculate the cell parameters and the average crystal size, by means of the MAUD computer program.[27] This program precisely takes into account the instrumental broadening resolution and performs the separation of the lattice strains contribution from the broadening originated as a result of crystallite size reduction. MAUD implemented a peak broadening description of the analytical Pseudo-Voigt lines, similarly to the pioneering Williamson Hall plot used in multiple profile analysis.[28]

SC-XRD Studies. Crystal data and collection details for 1·CH₂Cl₂ and **2** are listed in Table 3. The diffraction experiments were carried out on a Bruker APEX II diffractometer equipped with a CCD detector and using Mo-Kα radiation (λ = 0.71073 Å). Data were corrected for Lorentz polarization and absorption effects (empirical absorption correction SADABS).[29] The structures were solved by direct methods and refined by full-matrix least-squares based on all data using F^2.[30] All non-hydrogen atoms were refined with anisotropic displacement parameters. All hydrogen atoms were fixed at calculated positions and refined by a riding model, except N-bonded hydrogens which were preliminarily located in the Fourier difference map. Several restraints were applied to the C and N atoms

of 1·CH₂Cl₂ during refinement. In particular, all the atoms were restrained to have similar *U* parameters [SIMU command in SHELXL, s.u. 0.01]. Similar *U* restraints [SIMU command in SHELXL, s.u. 0.02] were applied to the C, O and N atoms of **2**. The crystals of **2** are pseudo-merohedrally twinned with twin matrix -1 0 0 0 -1 0 1 0 1 and refined batch factor 0.4254(13). The asymmetric unit of the unit cell of **2** contains three independent molecules (located on general positions), with very similar geometries and bonding parameters.

Table 3. Crystal data and details of the structure refinement for **1** and **2**.

	1·CH₂Cl₂	2
Formula	$C_{16}H_{88}Cl_8N_6O_9W_3$	$C_{10}H_{24}Cl_2N_4O_4W$
Fw	1293.67	519.08
λ, Å	0.71073	0.71073
Temperature, *K*	100(2)	100(2)
Crystal system	Orthorhombic	Monoclinic
Space group	$P2_12_12_1$	$P2_1/n$
a, Å	11.249(2)	14.211(3)
b, Å	11.476(2)	22.418(5)
c, Å	28.300(5)	18.094(4)
β, °	90	113.063(3)
Cell volume, Å³	3653.4(11)	5304(2)
Z	4	12
D_c, g cm⁻³	2.352	1.950
μ, mm⁻¹	10.055	6.854
F(000)	2424	3024
Crystal size	0.21×0.16×0.13	0.21×0.16×0.12
θ limits, °	1.44–26.00	1.22-26.00
Reflections collected	33756	51807
Independent reflections	7163 [$R_{int} = 0.0577$]	10547 [$R_{int} = 0.0830$]
Data / restraints / parameters	7163/ 129 / 379	10547 / 279 / 569
Goodness of fit on F^2	1.048	1.053
R1 ($I > 2σ(I)$)	0.0357	0.0544
wR2 (all data)	0.0726	0.1576
Largest diff. peak and hole, e.Å⁻³	2.100 / -1.502	2.445 / -3.752

Supplementary Material. Figures S1-S5 show P-XRD and HR-TEM representations, while Figure S6 and Tables S1-S2 show details related to DFT calculations. Cartesian coordinates of DFT-optimized compounds are collected in a separated .xyz file. CCDC reference numbers 1494264 (1·CH₂Cl₂) and 1494265 (2) contain the supplementary crystallographic data for the X-ray studies reported in this paper. These data can be obtained free of charge at www.ccdc.cam.ac.uk/conts/retrieving.html (or from the Cambridge Crystallographic Data Centre, 12, Union Road, CambridgeCB2 1EZ, UK; fax: (internat.) +44-1223/336-033; e-mail: deposit@ccdc.cam.ac.uk).

Computational studies. The computational geometry optimizations were carried out without symmetry constrains using the hybrid-GGA EDF2 functional,[31] in combination with the 6-31G** basis set (ECP-based LANL2DZ basis set for elements beyond Kr).[32] The "restricted" formalism was applied in all cases. The software used was Spartan 08. Further computational geometry optimizations were carried out without symmetry constrains, using the range-separated DFT functional ωB97X,[33] in combination with a polarized basis set composed by the 6-31G(d,p) set on the light atoms and the ECP-based LANL2TZ(f) on the metal centre.[34] The C-PCM implicit solvation model (ε = 9.08) was added to ωB97X calculations.[35] Gaussian '09 was used as software.[36] All the stationary points were characterized by IR simulations (harmonic approximation), from which zero-point vibrational energies and thermal corrections (T = 298.15 K) were obtained.[37] Vibrational simulation supported the interpretation of experimental IR data. Bond orders were estimated on the basis of Mayer's approach.[38] Cartesian coordinates of the optimized geometries are collected in a separated .xyz file.

References and Notes

1 (a) A. R. Armstrong, J. Canales and P. G. Bruce, *Angew. Chem., Int. Ed.*, 2004, **43**, 4899-4902. (b) (h) J. F. Ackerman, Mat. Res. Bull., 1988, **23**, 165-169. F. Madeira, S. Barroso, S. Namorado, P. M. Reis, B. Royo and A. M. Martins, *Inorg. Chim. Acta*, 2012, **383**, 152-156. (c) G. E. Buono-Core, A. H. Klahn, C. Castillo, M. J. Bustamante, E. Muñoz, G. Cabello and B. Chornik, *Polyhedron*, 2011, **30**, 201-206. (d) I. Cabrita, S. C. A. Sousa, A. C. Fernandes, *Tetrahedron Lett.*, 2010, **51**, 6132-6135. (e) I. Abrahams, J. L. Nowinski, P. G. Bruce and V. C. Gibson, *J. Solid State Chem.*, 1991, **94**, 254-259.

2 (a) R. Tia, E. Adei, J. Baidoo and J. Edor, *J. Chem. Sci.*, 2016, **128**, 707-718. (b) C. Wang and H. Yamamoto, *J. Am. Chem. Soc.*, 2014, **136**, 6888-6891. (c) Y.-L. Wong, L. H. Tong, J. R. Dilworth, D. K. P. Ng and H. Kay Lee, *Dalton Trans.*, 2010, **39**, 4602–4611. (d) K. Most, J. Hoßbach, D. Vidovic, J. Magull and N. C. Mösch-Zanetti, *Adv. Synth. Catal.*, 2005, **347**, 463–472. (e) Y.- L. Wong, D. K. P. Ng and H. K. Lee, *Inorg. Chem.*, 2002, **41**, 5276-5285.

3 (a) M. Epifani, T. Andreu, J. Arbiol, R. Diaz, P. Siciliano and J. R. Morante, *Chem. Mat.*, 2009, **21**, 5215-5221. (b) W. B. Cross, I. P. Parkin, A. J. P. White and D. J. Williams, *Dalton Trans.*, 2005, 1287-1293. (c) S. O'Neill, I. P. Parkin, R. J. H. Clark, A. Mills and N. Elliott, *Chem. Vapor Deposition*, 2004, **10**, 136-141. (d) M. Tong, G. Dai, Y. Wu, X. He and D. Gao, *J. Mat. Sci.*, 2001, **36**, 2535-2538.

4 See for instance: (a) S. Poongodi, P. S. Kumar, Y. Masuda, D. Mangalaraj, N. Ponpandian, C. Viswanathan and S. S. Ramakrishna, *RSC Adv.*, 2015, **5**, 96416-96427. (b) C. A. Bignozzi, S. Caramori, V. Cristino, R. Argazzi, L. Meda and A. Tacca, *Chem. Soc. Rev.*, 2013, **42**, 2228-2246. (c) E. Ozkan, S.-H. Lee, C. E. Tracy, P. Edwin, J. R. Pitts and S. K. Deb, *Solar Energy Mat. Solar Cells*, 2003, **79**, 439-448.

5 (a) J. Tillack, *Inorg. Synth.*, 1973, **14**, 109-122. (b) P. C. Crouch, G. W. A. Fowles and R. A. Walton, *J. Inorg. Nucl. Chem.*, 1970, **32**, 329-333.

6 V. C. Gibson, T. P. Kee and A. Shaw, *Polyhedron*, 1990, **9**, 2293-2298.

7 (a) I. Abrahams, J. L. Nowinski, P. G. Bruce and V. C. Gibson, *J. Solid State Chem.*, 1993, **102**, 140-145. (b) Von O. Jarchow, F. Schroder and H. Schulz, *Z. Anorg. Allg. Chem.*, 1968, **363**, 58-72.

8 (a) P. Dabas and M. K. Rastogi, *Asian J. Chem.*, 1997, **9**, 445-452. (b) B. J. Brisdon, *Inorg. Chem.*, 1967, **6**, 1791-1795.

9 Recent selected references are: (a) M. Bortoluzzi, E. Ferretti, F. Marchetti, G. Pampaloni, C. Pinzino and S. Zacchini, *Inorg. Chem.*, 2016, **55**, 4173−4182. (b) M. Bortoluzzi, M. Hayatifar, F. Marchetti, G. Pampaloni and S. Zacchini, *Inorg. Chem.*, 2015, **54**, 4047−4055. (c) M. Bortoluzzi, F. Marchetti, G. Pampaloni and S. Zacchini, *Dalton Trans.*, 2014, **43**, 16416–16423. (d) F. Marchetti, G. Pampaloni and C. Pinzino, *Chem. Eur. J.*, 2013, **19**, 13962-13969. (e) F. Marchetti and G. Pampaloni, *Chem. Commun.*, 2012, **48**, 635-653.

10 M. Bortoluzzi, F. Marchetti, G. Pampaloni and S. Zacchini, *Chem. Commun.*, 2015, **51**, 1323-1325.

11 (a) M. Bortoluzzi, F. Marchetti, G. Pampaloni, C. Pinzino and S. Zacchini, *Inorg. Chem.*, 2016, **55**, 887-893. (b) M. Bortoluzzi, F. Marchetti, G. Pampaloni and S. Zacchini, *Inorg. Chem.*, 2014, **53**, 3832-3838.

12 More reactive forms of solid compounds are often obtained at relatively low temperatures, see for instance: (a) F. Calderazzo, F. Masi and G. Pampaloni, *Inorg. Chim. Acta*, 2009, **362**, 4291–4297. (b) F. Calderazzo, G. De Benedetto, U. Englert, I. Ferri, G. Pampaloni and T. Wagner, *Z. Naturfosch.*, 1996, **51B**, 506-515. (c) T. A. Swaddle, *Inorganic Chemistry, An Industrial and Environmental Perspective*, Academic Press, 1991, p. 205.

13 See for instance: HgO, red and yellow forms. N. N. Greenwood and A. Earnshaw, *Chemistry of the Elements*, 2nd Ed., 1997, Elsevier, Amsterdam, pp. 1208-1209.

14 The high air sensitivity of grey WO_2Cl_2, leading to quick degradation, prevented a clear TEM analysis.

15 O. Yamaguchi, D. Tomihisa, H. Kawabata and K. Shimizu, *J. Am. Ceram. Soc.*, 1987, **70**, C94-C96.

16 R. J. Fante and P. E. Hoggard, *Trans. Metal Chem.*, 2008, **33**, 825-828.

17 G. R. Lee and J. A. Crayston, *J. Mat. Chem.*, 1996, **6**, 187-192.

18 P. Malinowski, Z. Mazej and W. Grochala, *Z. Anorg. Allg. Chem.*, 2008, **634**, 2608-2616.

19 (a) C. A. Dodds, M. D. Spicer and T. Tuttle, *Organometallics*, 2011, **30**, 6262-6269. (b) P. D. W. Boyd, M. G. Glenny, C. E. F. Rickard and A. J. Nielson, *Polyhedron*, 2011, **30**, 632-637. (c) Y.-L. Wong, L.-H. Tong, J. R. Dilworth, D. K. P. Ng and H. K. Lee, *Dalton Trans.*, 2010, **39**, 4602-4611. (d) M. F. Davis, W. Levason, M. E. Light, R. Ratnani, G. Reid, K. Saraswat and M. Webster, *Eur. J. Inorg. Chem.*, 2007, 1903-1910. (e) M. F. Davis, W. Levason, R. Ratnani, G. Reid, T. Rose and M. Webster, *Eur. J. Inorg. Chem.*, 2007, 306-313. (f) Y.-L. Wong, Q. Yang, Z.-Y. Zhou, H.-K. Lee, T. C. W. Mak and D. K. Ng, *New J. Chem.*, 2001, **25**, 353-357. (g) Y.-L. Wong, Y. Yan, E. S. H. Chan, Q. Yang, T. C. W. Mak and D. K. Ng, *J. Chem. Soc., Dalton Trans.*, 1998, 3057-3064.

20 (a) H. Sugimoto, M. Tarumizu, H. Miyake and H. Tsukube, *Eur. J. Inorg. Chem.*, 2007, 4663-4668. (b) W. A. Herrmann, G. M. Lobmaier and M. Elison, *J. Organomet. Chem.*, 1996, **520**, 231-234. (c) J. Sundermeyer, J. Putterlik, M. Foth, J. S. Field and N. Ramesar, *Chem. Ber.*, 1994, **127**, 1201-1212. (d) A. A. Eagle, C. G. Young and E. R. T. Tiekink, *Organometallics*, 1992, **11**, 2934-2938.

21 X. Ma, Z. Yang, C. Schulzke, M. Noltemeyer and H.-G. Schmidt, *Inorg. Chim. Acta*, 2009, **362**, 5275-5277.

22 J. F. de Wet, M. R. Caira and B. J. Gellatly, *Acta Crystallogr.*, 1978, **34B**, 762-766.

23 N. G. Connelly and W. E. Geiger, *Chem. Rev.*, 1996, **96**, 877-910.

24 W. Willker, D. Leibfritz, R. Kerssebaum and W. Bermel, *Magn. Reson. Chem.*, 1993, **31**, 287-292.

25 D. A. Skoog, D. M. West and F. J. Holler, Fundamentals of Analytical Chemistry, 7th Edition, Thomson Learning, Inc, USA, 1996.

26 J. Ayache, L. Beaunier, J. Boumendil, G. Ehret and D. Laub, *Sample Preparation Handbook for Transmission Electron Microscopy*, Springer, New York, 2010.

27 L. Lutterotti and S. Gialanella, *Acta Mater.*, 1998, **46**, 101-110.

28 W. H. Hall, *Proceed. Phys. Soc. Sect. A*, 1949, **62**, 741-743.

29 G. M. Sheldrick, SADABS, Program for empirical absorption correction, University of Göttingen, Göttingen, Germany, 1996.

30 G. M. Sheldrick, SHELX97, Program for crystal structure determination, University of Göttingen, Göttingen, Germany, 1997.

31 C. Y. Lin, M. W. George and P. M. W. Gill, *Aust. J. Chem.*, 2004, **57**, 365-370.

32 (a) M. Dolg, *Modern Methods and Algorithms of Quantum Chemistry*, J. Grotendorst Ed., John Neumann Institute for Computing, NIC series, Jülich, 2000, **3**, 507-540. (b) P. J. Hay and W. R. Wadt, *J. Chem. Phys.*, 1985, **82**, 270-283. (c) P. J. Hay and W. R. Wadt, *J. Chem. Phys.*, 1985, **82**, 299-310. (d) W. J. Henre, R. Ditchfield and J. A. Pople, *J. Chem. Phys.*, 1972, **56**, 2257-2261.

33 (a) Y. Minenkov, Å. Singstad, G. Occhipinti and V. R. Jensen, *Dalton Trans.*, 2012, **41**, 5526-5541. (b) J.-D. Chai and M. Head-Gordon, *Phys. Chem. Chem. Phys.*, 2008, **10**, 6615-6620. (c) I. C. Gerber and J. G. Ángyán, *Chem. Phys. Lett.*, 2005, **415**, 100-105.

34 (a) L. E. Roy, P. J. Hay and R. L. Martin, *J. Chem. Theory Comput.*, 2008, **4**, 1029-1031. (b) M. M. Francl, W. J. Pietro, W. J. Hehre, J. S. Binkley, D. J. DeFrees, J. A. Pople and M. S. Gordon, *J. Chem. Phys.*, 1982, **77**, 3654-3665.

35 (a) M. Cossi, N. Rega, G. Scalmani and V. Barone, *J. Comput. Chem.*, 2003, **24**, 669-681. (b) V. Barone and M. Cossi, *J. Phys. Chem. A*, 1998, **102**, 1995-2001.

36 Gaussian 09, Revision C.01, M. J. Frisch et al., Gaussian, Inc., Wallingford CT, 2010.

37 C. J. Cramer, *Essentials of Computational Chemistry,* 2nd Edition, Wiley, Chichester, 2004.

38 (a) A. J. Bridgeman, G. Cavigliasso, L. R. Ireland and J. Rothery, *J. Chem. Soc., Dalton Trans.*, 2001, 2095-2108. (b) I. Mayer, *Int. J. Quantum Chem.*, 1984, **26**, 151-154.